BJP British Journal of Pharmacology

DOI:10.1111/bph.12459
www.brjpharmacol.org

RESEARCH PAPER

The protein Ocular albinism 1 is the orphan GPCR GPR143 and mediates depressor and bradycardic responses to DOPA in the nucleus tractus solitarii

Y Hiroshima[1,2], H Miyamoto[1,2], F Nakamura[2], D Masukawa[2], T Yamamoto[2], H Muraoka[2], M Kamiya[2], N Yamashita[2], T Suzuki[3], S Matsuzaki[4], I Endo[1] and Y Goshima[2]

[1]*Department of Gastroenterological Surgery, Yokohama City University Graduate School of Medicine, Yokohama, Japan,* [2]*Department of Molecular Pharmacology and Neurobiology, Yokohama City University Graduate School of Medicine, Yokohama, Japan,* [3]*Department of Child Development, Hoshi University School of Pharmacy and Pharmaceutical Sciences, Tokyo, Japan, and* [4]*Graduate School of Medicine, Osaka University, Osaka, Japan*

Correspondence
Y Goshima, Department of Molecular Pharmacology and Neurobiology, Yokohama City University Graduate School of Medicine, 3-9 Fukuura, Kanazawa-ku, Yokohama 236-0004, Japan. E-mail: goshima@med.yokohama-cu.ac.jp

Keywords
L-3; 4-dihydroxyphenylalanine; neurotransmitter; baroreceptor reflex; nucleus tractus solitarii; G-protein coupled receptor

Received
12 May 2013
Revised
12 September 2013
Accepted
30 September 2013

BACKGROUND AND PURPOSE

L-DOPA is generally considered to alleviate the symptoms of Parkinson's disease by its conversion to dopamine. We have proposed that DOPA is itself a neurotransmitter in the CNS. However, specific receptors for DOPA have not been identified. Recently, the gene product of *ocular albinism 1* (OA1) was found to exhibit DOPA-binding activity. Here, we have investigated whether OA1 is a functional receptor of DOPA in the nucleus tractus solitarii (NTS).

EXPERIMENTAL APPROACH

We examined immunohistochemical expression of OA1 in the NTS, and the effects of DOPA microinjected into the depressor sites of NTS on blood pressure and heart rate in anaesthetized rats, with or without prior knock-down of OA1 in the NTS, using shRNA against OA1.

KEY RESULTS

Using a specific OA1 antibody, OA1-positive cells and nerve fibres were found in the depressor sites of the NTS. OA1 expression in the NTS was markedly suppressed by microinjection into the NTS of adenovirus vectors carrying the relevant shRNA sequences against OA1. In animals treated with OA1 shRNA, depressor and bradycardic responses to DOPA, but not those to glutamate, microinjected into the NTS were blocked. Bilateral injections into the NTS of DOPA cyclohexyl ester, a competitive antagonist against OA1, suppressed phenylephrine-induced bradycardic responses without affecting blood pressure responses.

CONCLUSION AND IMPLICATIONS

OA1 acted as a functional receptor for DOPA in the NTS, mediating depressor and bradycardic responses. Our results add to the evidence for a central neurotransmitter role for DOPA, without conversion to dopamine.

Abbreviations

AADC, aromatic L-amino acid decarboxylase; DOPA CHE, DOPA cyclohexyl ester; NTS, nucleus tractus solitarii; OA1, ocular albinism 1; TH, tyrosine hydroxylase

Introduction

Since being established as a precursor for catecholamine biosynthesis, DOPA has been believed to be a pharmacologically inert amino acid that alleviates the symptoms of Parkinson's disease via its conversion to dopamine by the enzyme aromatic L-amino acid decarboxylase (AADC) (Bartholini *et al.*, 1967). However, in the course of our study measuring endogenous catecholamines released from superfused rat brain slices (Goshima *et al.*, 1986), we found that the amount of DOPA in the superfusate fractions was increased during electrical field stimulation (Goshima *et al.*, 1988). We conducted a series of experiments to address whether DOPA fulfils the criteria for a neurotransmitter, such as synthesis, metabolism, active transport, existence, physiological release, competitive antagonism and physiological or pharmacological responses (Misu and Goshima, 1993; Misu *et al.*, 2003). There are neurons that synthesize DOPA and that are positive for tyrosine hydroxylase (TH) but AADC negative (Okamura *et al.*, 1988; Yue *et al.*, 1994). Sodium ion-dependent [^{3}H]-DOPA uptake has been detected in neurons and in the CNS (Sugaya *et al.*, 2001). DOPA is released on electrical stimulation in a tetrodotoxin-sensitive and Ca^{2+}-dependent manner (Goshima *et al.*, 1988).

The baroreceptor reflex is the principal neuronal mechanism by which the cardiovascular system is regulated under a negative control. The primary baroreceptor afferents, the carotid sinus nerve and aortic depressor nerve terminate in depressor sites of the nucleus tractus solitarii (NTS) (Talman *et al.*, 1980; Andresen and Mendelowitz, 1996; Sun, 1996; Aicher *et al.*, 2000). Even after treatment with an AADC inhibitor, DOPA microinjected into the NTS induced depressor and bradycardic responses in anaesthetized rats (Kubo *et al.*, 1992; Yue *et al.*, 1994). This action was not mimicked by a similar dose of dopamine (Kubo *et al.*, 1992). Furthermore, the depressor and bradycardic responses to DOPA were blocked by DOPA methyl ester, the first competitive antagonist for DOPA (Goshima *et al.*, 1991; Kubo *et al.*, 1992). Based on these and other findings, we suggested that DOPA itself is a neurotransmitter, in addition to being a precursor of dopamine.

In spite of extensive efforts (Aoki *et al.*, 2011), identification of the specific receptor(s) for DOPA was unsuccessful. Recently, the protein ocular albinism 1 (OA1), one of the orphan GPCRs also known as GPR143, (receptor nomenclature follows Alexander *et al.*, 2013), was shown to possess DOPA-binding activity and could function as a DOPA receptor in retinal pigment epithelium cells (Lopez *et al.*, 2008). OA1 is the protein product of the *oa1* gene (Schiaffino *et al.*, 1999)and mutation of the *oa1* gene causes ocular albinism type 1, an X-linked disorder characterized by severe reduction of visual acuity, retinal hypopigmentation, foveal hypoplasia, optic misrouting and the presence of giant melanosomes in skin melanocytes and retinal pigment epithelium (O'Donnell *et al.*, 1976; Garner and Jay, 1980). In this study, we have investigated whether OA1 plays a role as the receptor mediating the responses to DOPA in the NTS. On the basis of the results obtained in this study, we now propose that OA1 is a receptor that mediates depressor and bradycardic responses to DOPA in the NTS.

Methods

Cell culture

COS-7, CHO and ARPE-19 cells were obtained from American Type Culture Collection (Manassas, VA, USA). COS-7 and ARPE-19 cells were cultured in DMEM. CHO cells were cultured in F-12 Ham medium. These media were supplemented with 10% FBS, penicillin (100 U·mL^{-1}) and streptomycin (100 μg·mL^{-1}), and incubated at 37°C in a humidified atmosphere with 5% CO_2.

Plasmid construction

The entire coding region of mouse OA1 was real-time PCR (RT-PCR) amplified with two primers (atcgaattccgaATGGC CTCCCCGCGCCTGGGAATTTTC and atcctcgagTCAGAGTT CCCCCTGGGCTTGGGAAATGGA) and cloned into psNmyc vector, which contains the N-terminal Ig κ secretion signal and myc epitope. To generate an expression vector for OA1-EGFP, mouse OA1 coding region attached with Ig κ secretion signal was inserted into pEGFP-N3 (Clontech, Mountain View, CA, USA). OA1-mCherry was also constructed by the replacement of EGFP coding fragment with mCherry. psNmyc vector and mCherry vector were kindly provided by Dr H Usui and Professor R Y Tsien (UCSD) respectively. All cDNAs were verified by sequencing.

Antibody preparation

An antiserum against rat OA1 was raised by injection of the peptide (CSAAEGTYQTPEGS, 335-348AA) conjugated with keyhole limpet hemocyanin into rabbits. The serum was collected and the specific antibodies were affinity purified by the antigen peptide affinity column and dialysed against PBS, pH 7.4.

Immunoblot analysis

COS-7 cells were cultured for 24 h, and transfected with Myc-OA1 expression vector using FuGENE transfection reagent (Promega). After 48 h, COS-7 cells were lysed in immunoprecipitation buffer (20 mM Tris-HCl, pH 8.0, 150 mM NaCl, 1 mM EDTA, 10 mM NaF, 1 mM Na_3VO_4, 1% Nonidet P-40 and 50 μM ρ-amidinophenylmethanesulfonyl fluoride). The lysates were centrifuged at 20 000 × *g* for 10 min at 4°C, and supernatants were dissolved in SDS 4× sample buffer containing dithiothreitol (50 mM). The samples were then used for immunoblot analysis of anti-OA1 (diluted 1:1000) antibodies. After probing with the primary antibodies, the membrane was washed and incubated with the secondary anti-rabbit IgG antibody coupled to HRP (GE Healthcare). The antibody-antigen complexes were identified with Western Chemiluminescent HRP Substrate (Millipore).

Animals

All animal care and experimental procedures were conducted in accordance with NIH guidelines concerning the Care and Use of Laboratory Animals and with the approval of the Animal Care Committee of the Yokohama City University Graduate School of Medicine. Throughout the experimental procedures, all efforts were made to minimize the number of animals used and their suffering. All studies involving

animals are reported in accordance with the ARRIVE guidelines for reporting experiments involving animals (Kilkenny *et al.*, 2010; McGrath *et al.*, 2010). A total of 40 animals were used in the experiments described here. Post-natal day 15 (P15) Wistar rats (Charles River Laboratories) were used for immunohistochemical analysis. Adult male Wistar rats (240–350 *g*; Charles River Laboratories) were used for the shRNA knock-down and blood pressure (BP) and heart rate (HR) monitoring (see below).

Immunocytochemistry and immunohistochemistry

Twenty four hours after transfection with OA1-mCherry as described above, COS-7 cells were fixed with paraformaldehyde (PFA; 4%)/PBS (pH 7.4) at room temperature for 10 min and then blocked for 1 h in Tween-Tris buffered saline [137 mM NaCl, 2.68 mM KCl, 25 mM Tris base, 0.01% Tween20 (TBST)] containing 10% normal goat serum. The cells were incubated with anti-OA1 antibody at 4°C for 24 h, and then incubated with Alexa 488 conjugated goat anti-mouse IgG (Invitrogen). Rats (P15) were deeply anaesthetized with isoflurane and perfused intracardially with 4% FA in PBS, pH 7.4. The brains were removed, and post-fixed in 4% PFA overnight. After being cryoprotected with 30% sucrose, the brains were embedded with Tissue-Tek O.C.T. Compound (Sakura Finetechnical), and coronally sliced (16 µm thick). Cryostat serial sections were heat treated at 70°C for 20 min in Histo VT One (Nacalai Tesque). Sections were then treated with 0.1% Triton X-100 in TBST for 10 min and with 0.3% H_2O_2 for 30 min at room temperature. Immunostaining was performed according to a standard avidin/biotin peroxidase protocol (Vectastain Elite ABC kit) using anti-OA1 antibody and anti-TH rabbit polyclonal antibody (diluted 1:300; Chemicon Inc., Temecula, CA, USA). Specific labelling was visualized with the 3,3′ diaminobenzidine kit (DAKO Cytomation). The peptide competition assay was performed for confirming the specific staining reactivity of the antibody. The antibody was pre-incubated with the peptide prior to use in immunostaining. All other parameters of the immunostaining experiment were the same.

Construction of recombinant adenoviruses

The specific short hairpin RNA (shRNA) sequence for *oa1* RNAi (gatccgATACTCAGCACCTCATCAGAAGTGTttcaagagaACACTTCTGATGAGGTGCTGAGTATttttttGAATTCa) and the scramble short hairpin RNA sequence (gatccgGAACCTCTTCGAACGACTATTGACAttcaagagaTGTCAATAGTCGTTCGAAGAGGTTCttttttGAATTCa) were inserted into the pRNAT-H1.1/Shuttle vector (GenScript), which carries coral GFP (cGFP) under CMV promoter control to track the transfection efficiency. Each shRNA sequence coding region was transferred into the Adeno-X viral DNA. Recombinant adenovirus vector was generated according to the instructions of the manufacturer (Clontech). The titer of a recombinant adenovirus that contained a specific shRNA sequence for *oa1* RNAi (*oa1*-Ad) was 1.52×10^{10} virus particles (VP) mL^{-1}, and that of a recombinant adenovirus containing the scramble shRNA sequence (scramble-Ad) was 1.01×10^{10} VP mL^{-1}.

In vivo *adenovirus gene transfer to the eye and the NTS*

Rats (P15) were anaesthetized with urethane (1.2 $g \cdot kg^{-1}$, i.p.). The *oa1*-Ad (7.60×10^6 VP 50 μL^{-1}) or scramble-Ad (5.05×10^6 VP 50 μL^{-1}) was microinjected into the eyeball. Forty-eight hours after injection, the eyeballs were removed and post-fixed in 4% PFA overnight. After being cryoprotected with 30% sucrose, the eyeballs were embedded with Tissue-Tek O.C.T. Compound, and sagittally sliced (10 µm thick) for immunohistochemistry. Before gene transfer to the NTS, anaesthetized rats were placed in a stereotaxic apparatus with the head fixed at 45°. The dorsal surface of the lower brainstem was exposed by a limited occipital craniotomy. A glass micropipette pulled to an outside tip diameter of 50–100 µm was introduced into the NTS (0.6 mm rostral and 0.6 mm lateral to the caudal tip of the area postrema and 0.6 mm beneath the dorsal surface of the brainstem) (Kubo *et al.*, 1992). After identifying the depressor site of the NTS with the microinjection of *L*-glutamate, the *oa1*-adenovirus (1.52×10^4 VP 100 nL^{-1}) was unilaterally microinjected into the depressor site, and the scramble-adenovirus (1.01×10^4 VP 100 nL^{-1}) into the other side of the depressor site. The wound was sutured and cleaned, and the rats were allowed to recover in their cages. Buprenorphine hydrochloride (Reckitt Benckiser Pharmaceuticals, Richmond, VA, USA), 0.05 $mg \cdot kg^{-1}$ s.c., was given when the behavioural signs of post-operative pain were detected. Forty-eight hours after microinjection of *oa1*- or scramble-Ad, rats with no infections around the wound, no signs of rough coats, loss of weight and of lethargy post-operatively, were used to test the effects of DOPA microinjected into the NTS. The expression of OA1 and cGFP were detected by anti-OA1 antibody and anti-GFP chicken polyclonal antibody (AVES). For normalized quantitative analysis of OA1 immunohistochemistry, the ratio between OA1 and cGFP intensity was calculated in each cell expressing both OA1 and cGFP in the NTS using ImageJ software. Data from any injection sites outside that range were not analysed in our experiments.

RT-PCR

At the end of experiments, the injection site was marked by injecting 100 nL of Evans Blue dye solution. The brains were removed and preserved in liquid nitrogen. The $2 \times 2 \times 2$ mm^3 fragment including the injection site was taken out from the frozen brain tissue and homogenized using TRIzol (Invitrogen). Total RNA was extracted after homogenization of tissue samples, followed by on-column clean-up with the RNA spin mini kit (GE Healthcare BioSciences). Total RNA (2 µg) was reverse transcribed with the High Capacity RNA-to-cDNA Kit (Applied Biosystems, Foster City, CA, USA) for cDNA synthesis. PCRs were performed in 20 µL reactions containing 2 µL cDNA, 10 µL 2 × Universal TaqMan PCR Master Mix (Applied Biosystems) and 2 µL of Assays-on-Demand TaqMan Gene Expression Probes (Applied Biosystems). The probes used were *oa1* (Rn01771058_m1) and GAPDH as an endogenous control (Rn99999916_s1). All reactions were performed in triplicate using the ABI 7900 HT Fast (Applied Biosystems) according to the following thermal cycle protocol: 95°C for 20 s, followed by 40 cycles of 95°C for 1 s and 60°C for 20 s. The GAPDH transcript level was used to normalize gene expression levels.

Microinjection of DOPA into the NTS

Adult male Wistar rats (240–350 *g*; Charles River Laboratories) were anaesthetized with urethane (1.2 g·kg^{-1}, i.p.). The femoral artery and vein were cannulated for recording systolic/diastolic BP and for i.v. infusion respectively (Kubo *et al.*, 1992). Rats were paralysed with *d*-tubocurarine (1 mg·kg^{-1}, i.m.), artificially ventilated with a respirator, and placed in a stereotaxic apparatus with the head fixed at 45°. The dorsal surface of the lower brainstem was exposed by a limited occipital craniotomy. A glass micropipette was introduced into the NTS as described above. DOPA (60 ng) and glutamate (100 ng) dissolved in saline were injected unilaterally into the NTS in a volume of 50 nL in 2 s. DOPA cyclohexylester (DOPA CHE) (1 μg), when used, was injected ipsilaterally or bilaterally into the NTS in a volume of 50 nL in 2 s on each side. To identify the depressor sites, we microinjected glutamate into the depressor sites, and confirmed the depressor and bradycardic responses before the DOPA microinjection. Phenylephrine was infused (15 μg 10 mL^{-1}·min^{-1} for 15 s, i.v.) 10 min after the bilateral application of DOPA CHE into the NTS. At the end of experiments, the injection site was marked by injecting 100 nL of Evans Blue dye solution. The brains were removed, frozen serial sections were cut (20 μm) with a cryostat (Leica, Wetzlar, Germany) and the sites were identified. Data from any injection sites outside that range were not analysed in our experiments.

Radiolabelled ligand binding

CHO cells expressing OA1-EGFP were plated into 10 cm culture dishes. Cells were chilled on ice and then rinsed in cold binding buffer, 25 mM Tris, 150 mM NaCl, 5 mM EDTA (pH 7.45). Cells were suspended to 0.5 × 10^6 cells mL^{-1} and incubated on ice for 2 h in the binding buffer supplemented with [^{3}H]-DOPA (American Radiolabeled Chemicals). The cells were washed with the chilled binding buffer five times. Specific binding values of [^{3}H]-DOPA to CHO cells expressing OA1-EGFP were estimated by subtracting the value of [^{3}H]-DOPA binding to CHO cells in the presence of DOPA CHE (10 mM).

Ca^{2+} Imaging

ARPE-19 cells transiently expressing mouse OA1-mCherry plated on glass coverslips were rinsed in Ca^{2+}-containing HEPES-buffered HBSS (pH 7.0) and then incubated with 2.5 μM Fura-2 (solubilized in anhydrous DMSO and 0.01% pluronic acid) for 30 min at 37°C, 5% CO_2. Fura-2-loaded cells were washed with 1 mL of HBSS four times. Each coverslip was incubated in 1 mL of HBSS in a chamber held at 37°C on the stage of an inverted Olympus IX71 microscope equipped with a UAPo/340 20× objective. Using a filter wheel, excitation light from a 200 W Xe bulb was passed alternately through 340 and 380 nm filters. A 30 nm bandpass filter, centred at 510 nm, selected for the emitted fluorescence that was passed to a CCD camera (Cool SNAP HQ).

Data analysis

The paired two-tailed Student's *t*-test was used to compare the variables of RT-PCR and the changes in BP and HR induced by DOPA, glutamate or phenylephrine. The unpaired two-tailed Student's *t*-test was used to compare other sets of data. In the text and figures, the results are presented as means ± SEM of *n* observation. *P*-values of less than 0.05 were considered statistically significant.

Materials

DOPA CHE was synthesized in Drug Discovery Laboratories, Research Institute, Kyowa Hakko Kogyo. DOPA and glutamate (monosodium salt) were purchased from Nacalai Tesque (Kyoto, Japan). Phenylephrine was purchased from Sigma Chemical (St Louis, MO, USA).

Results

Immunoblot analysis and immunocytochemistry with anti-OA1 antibody of COS7 cells expressing Myc-OA1 or OA1-mCherry

To characterize the anti-OA1 antibody generated in our study, we performed immunoblot analysis of COS7 cells expressing Myc-tagged mouse OA1. In immunoblot analysis using anti-OA1 antibody, 45, 80 kDa and higher molecular weight bands were detected (Figure 1A). These bands were blocked by the synthetic OA1 peptide immunogen (Figure 1A). The predicted molecular weight of Myc-OA1 is 45 kDa. The higher molecular weight bands may reflect glycosylation and/or homo- and hetero-oligomeric complexes of OA1. Indeed, it is well recognized that GPCR dimerization may be a requisite for function (Milligan, 2009). In samples boiled for 5 min at 100°C, several bands higher than 200 kDa were detected, suggesting that heat denaturation may accelerate aggregation of OA1. To examine whether this anti-OA1 antibody was applicable for immunocytochemistry, cultured COS7 cells expressing OA1-mCherry were fixed, and OA1-mCherry expressed was detected with anti-OA1 antibody and mCherry fluorescence. OA1-positive signals were observed in COS7 expressing OA1-mCherry, and these signals were blocked by the synthetic OA1 peptide immunogen (Figure 1B). Immunohistochemical examination also revealed that OA-1 was expressed in the retinal pigment epithelium cell layers (Figure 1C), a result consistent with previous reports (Schiaffino *et al.*, 1999; Surace *et al.*, 2000; Lopez *et al.*, 2008). Microinjection of *oa-1*-adenovirus vector but not ther scramble- adenovirus into the eye decreased the levels of OA1 expressed in the rat retinal pigment epithelium cells (Figure 1C). Thus, the anti-OA1 antibody was useful for detection of OA1 in immunoblot analysis and immunocytochemistry.

OA1 was expressed in the NTS and the median eminence of the hypothalamus

Next we performed immunohistochemical analysis and examined the distribution of OA1 immunoreactive cells in the rat NTS and hypothalamus (Figure 2A–E). In the coronal section at the level of the obex (Figure 2A–E), we observed OA1-immunoreactive cells in the medial NTS (Figure 2B,C). The signals were inhibited by the synthetic OA1 peptide immunogen (Figure 2D). In the NTS, some cells labelled immunocytochemically with TH, a L-DOPA-forming enzyme

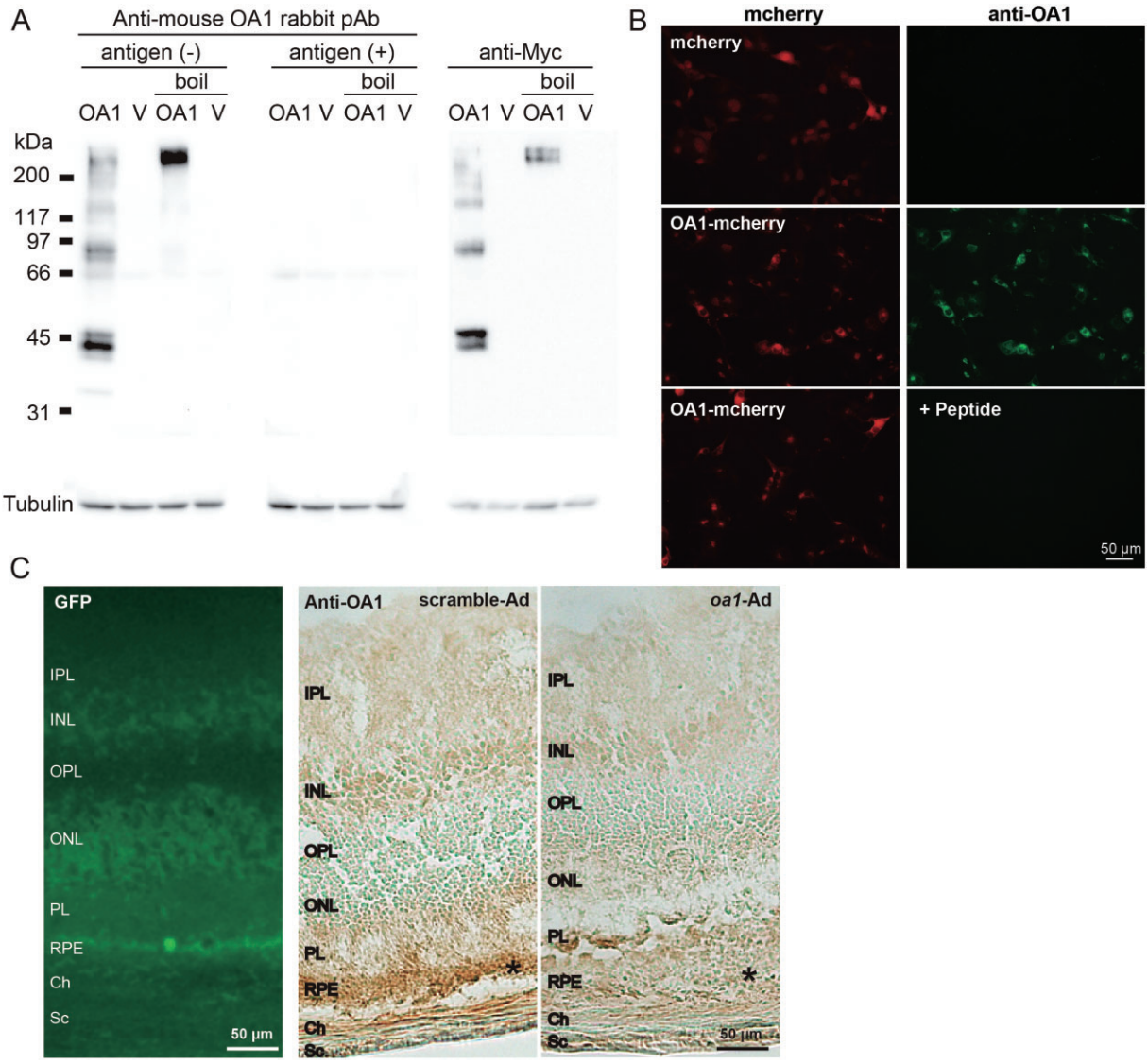

Figure 1

(A) Immunoblot analysis of COS-7 cells expressing Myc-tagged mouse OA1 expression vector (OA1) or empty vector (V) with anti-OA1 rabbit antibody or anti-Myc antibody. The anti-OA1 antibody recognized the 42, 80 kDa and higher molecular weight bands in the OA1-expressing cell lysates without heat denaturation. In samples boiled for 5 min at 100°C, several bands higher than 200 kDa were detected, suggesting that heat denaturation caused aggregation of OA1. These immunoreactive bands were blocked by synthetic OA1 C-terminal peptide (314-405AA) including the immunogen sequence. Similar immunoreactive bands appeared with anti-Myc antibody. The size of 42 kDa correlates well with the deduced molecular weight of mouse OA1 protein from the cDNA sequence. The higher molecular weight bands may reflect glycosylation and/or homo- and hetero-oligomeric complexes of OA1. The similar amount of protein loading was confirmed by tubulin immunoblotting (lower panels). (B) OA1-mCherry expression in COS7 cells was detected by anti-OA1 antibody and mCherry fluorescence. Immunofluorescence of OA1 detected in mCherry-positive cells was blocked by the synthetic OA1 peptide. (C) Immunohistochemical localization of OA1 in rat retinae infected with *oa1* and scramble vectors. cGFP was monitored to track the transfection efficiency (left). The expression of OA1 in retinal pigment epithelium (RPE) indicated by the asterisk (*) was significantly suppressed by *oa1*-Ad injection. IPL: inner plexiform layer, INL: inner nuclear layer, OPL: outer plexiform layer, ONL: outer nuclear layer, PL: photoreceptor layer, Ch: choroid, Sc: sclera. Immunohistochemical examination was performed 48–72 h after infection of rat retinae with the adenoviral constructs. Scale bar, 50 µm.

(Yue *et al.*, 1994). To examine the relationships between OA1-positive and TH-positive neurons, we also performed immunohistochemical examination with anti-TH antibody. As with the OA1-immunoreactive cells, TH-immunoreactive neurons were observed in the medial NTS (Figure 2E). We also showed DOPA-containing neurons and DOPA uptake sites in the hypothalamic areas (Sugaya *et al.*, 2001). Consistent with these data, OA1 immunoreactive cells were detected in the hypothalamic median eminence (Figure 2G,H). No immunoreactive material was detected with pre-absorbed antisera.

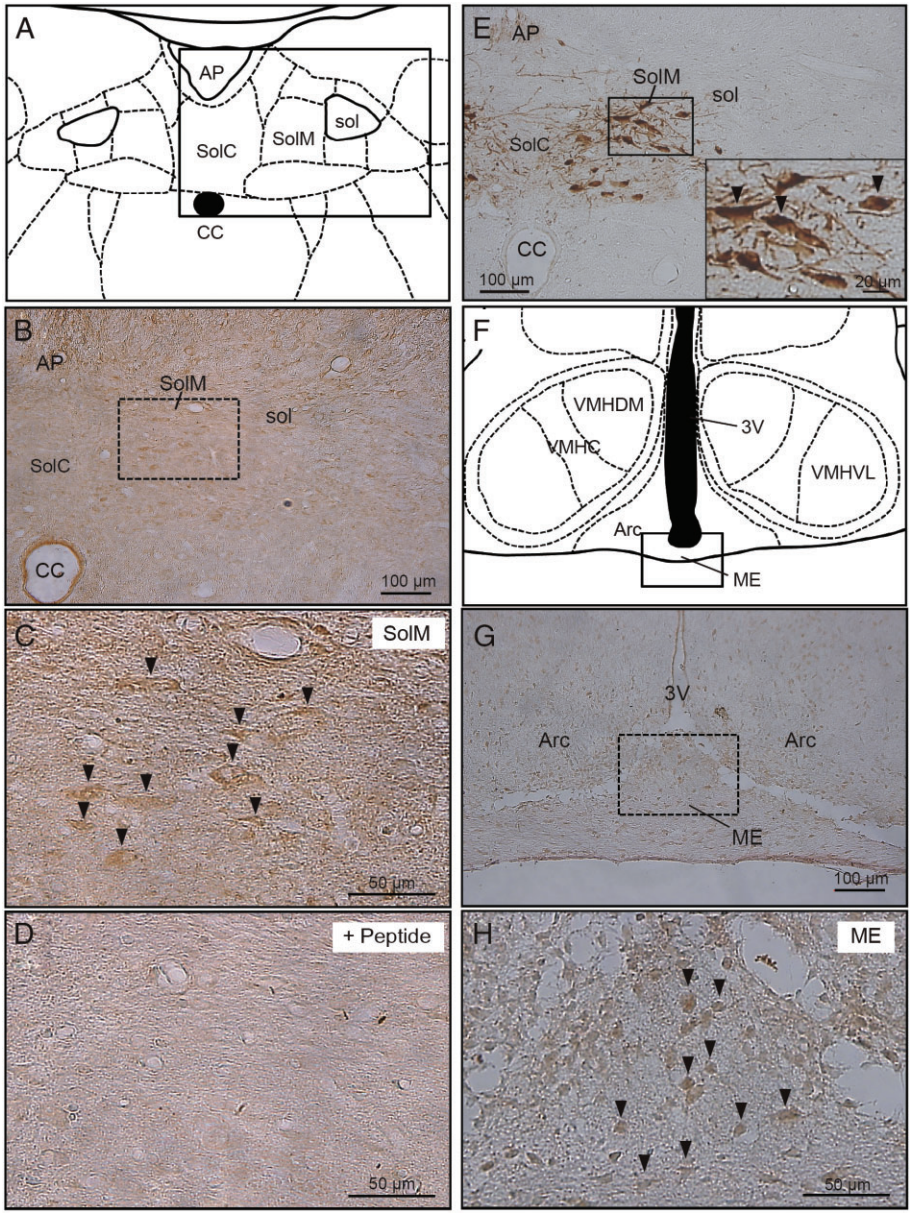

Figure 2

(A) Diagram of rat medulla oblongata in a coronal section. Image of boxed area in (A) is shown in (B). CC: central canal, AP: area postrema, SolM: nucleus of solitary tract medial, SolC: commissural, sol: solitary tract. (B) The coronal section of rat medulla oblongata immunostained with anti-OA1 antibody. Magnified image of boxed area in (B) is shown in (C). (D) The OA1 signals were inhibited by the peptide immunogen against the OA1 antibody. (E) The coronal section of rat medulla oblongata was immunostained with anti-TH antibody. Arrowheads in a magnified image (right lower panel) of boxed area indicate the cells positively stained with anti-TH antibody. (F) Diagram of rat hypothalamus in a coronal view. Image of boxed area in (F) is shown in (G). VMHDM: nucleus of ventromedial hypothalamus dorsomedial, VMHC: central, VMHVL: ventrolateral, Arc: arcuate nucleus, ME: median eminence, 3V: third ventricle. (G) The coronal section of rat hypothalamus was immunostained with anti-OA1 antibody. Magnified image of boxed area in (G) is shown in (H). Arrowheads indicate the cells positively stained with anti-OA1 antibody. These signals were inhibited by the peptide immunogen (data not shown).

Introducing oa1-specific shRNA into the NTS suppressed expression of OA1 in the NTS and attenuated the depressor and bradycardic responses to DOPA, but not to glutamate

Again, we performed knock-down experiment on OA1 in the NTS of adult rats to confirm that OA1 was expressed in the NTS. Efficiency of the adenoviral infection was monitored by co-expression of cGFP. We confirmed the effects of *oa1*-adenovirus on the expression of OA1 mRNA in the NTS by RT-PCR (Figure 3A). The expression of OA1 mRNA in the NTS regions including the injection sites of *oa1*-adenovirus was significantly suppressed when compared with the injection sites of scramble-adenovirus. Immunohistochemical analysis

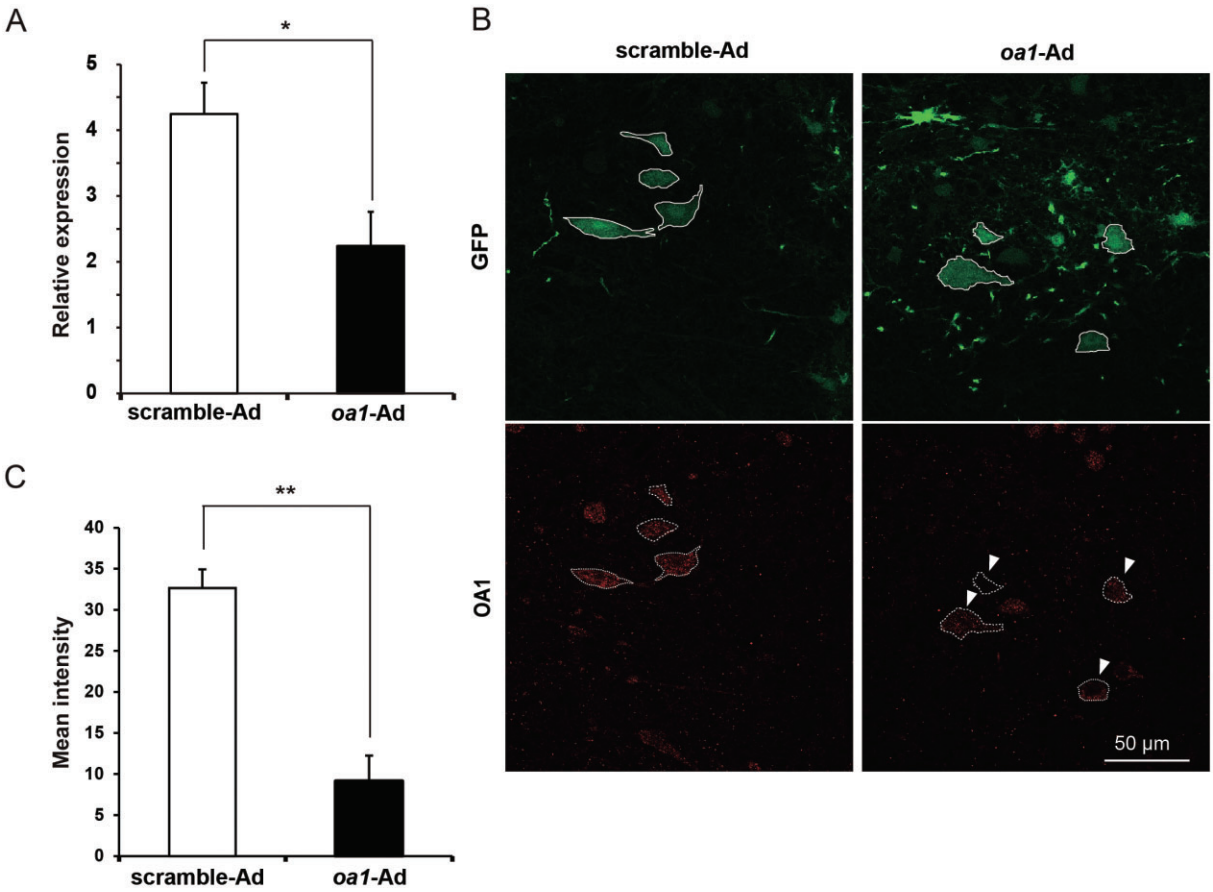

Figure 3

(A) Quantitative RT-PCR analysis of the expression of OA1 mRNA in the NTS infected with scramble- and *oa1*-adenovirus vectors. The expression of OA1 was suppressed in the side injected with *oa1*-adenovirus (*oa1*-Ad). *$P < 0.05$, compared with scramble-adenovirus (scramble-Ad); ($n = 5$). (B) Immunohistochemical localization of OA1 in the NTS injected with scramble- and *oa1*-adenovirus vectors. The immunofluorescence levels of OA1 in the NTS injected with *oa1*-adenovirus vector were suppressed, compared to that with scramble-adenovirus vector. (C) Quantitative analysis of the effect of *oa1*-adenovirus vector injection. The ratio between OA1 and cGFP immunofluorescence level was calculated in each cell expressing OA1 and cGFP. **$P < 0.01$, compared with the levels of the scramble side ($n = 11$–13).

also showed that the expression of OA1 was decreased in the NTS in the *oa1*-adenovirus injection sites (Figure 3B,C). The suppression of immunofluorescence levels of OA1 by microinjection of *oa1*-adenovirus into the NTS further supports the reliability of the anti-OA1 antibody.

Introducing scramble-adenovirus into the NTS did not affect depressor and bradycardic responses to either DOPA or glutamate (Figure 4A). Introducing *oa1*-adenovirus into the NTS attenuated the depressor and bradycardic responses to DOPA, without modifying the responses to glutamate (Figure 4B). These results indicated that OA1 in the NTS mediated depressor and bradycardic responses to DOPA, but not to glutamate (Figure 4C,D).

To determine whether OA1 plays a role in mediating baroreceptor reflex, we attempted to perform bilateral knockdown of OA1 in the NTS. Bilateral injection of *oa1*-Ad into the NTS, however, was associated with a high mortality rate of 80% (four out of five experiments) 24 to 48 h after the injection, while the injection of scramble-Ad did not (data not shown).

Displacement of the specific binding of [^{3}H]-DOPA by DOPA CHE, and DOPA-induced intracellular Ca^{2+} response

In our study, we therefore used DOPA CHE as a tool to investigate possible role of OA1 in the baroreceptor reflex. We previously reported that pretreatment with DOPA CHE blocked the depressor and bradycardic response to DOPA microinjected into the NTS (Furukawa *et al.*, 2000). To investigate whether DOPA CHE acted as an OA1 ligand, we first conducted binding experiment with [^{3}H]-DOPA in CHO cells expressing mouse OA1. Specific and saturable binding of [^{3}H]-DOPA was observed in OA1-EGFP-expressing CHO cells, but not in EGFP-transfected CHO cells. We determined the specific binding of [^{3}H]-DOPA by subtracting total minus non-specific binding. Non-specific binding of [^{3}H]-DOPA was obtained in the presence of 10 mM DOPA CHE. We confirmed that the specific binding of [^{3}H]-DOPA estimated by difference between the amount of [^{3}H]-DOPA in OA1-expressing and non-expressing cells was comparable to that

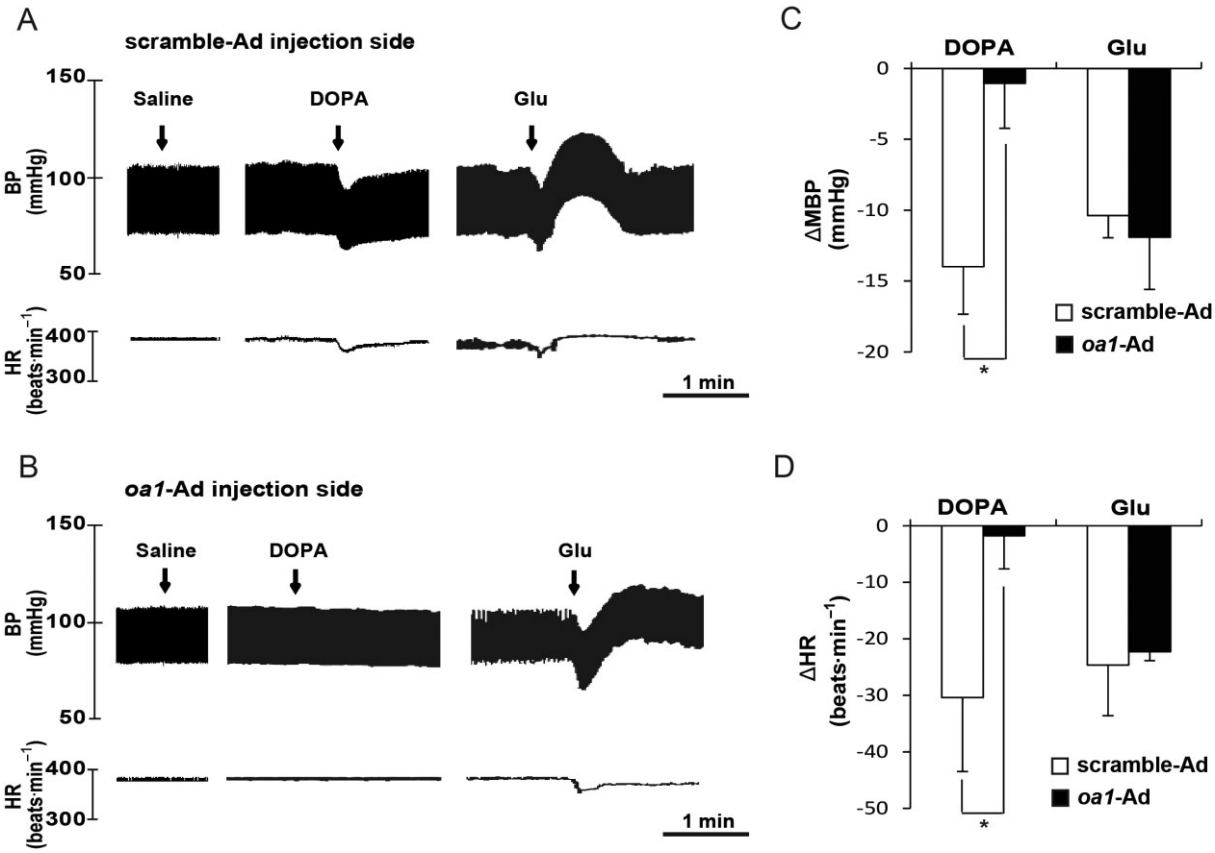

Figure 4

(A,B) Typical traces of the effects of DOPA (60 ng) and glutamate (Glu) (100 ng) microinjected into the right or left NTS infected with scramble- (scramble-Ad) or *oa1*-adenovirus (*oa1*-Ad) vectors on BP and HR in anaesthetized rats. In the scramble side, the depressor and bradycardic responses to DOPA were detected, whereas these responses were suppressed in the side injected with *oa1*-adenovirus. Responses to glutamate were detected in the *oa1*-adenovirus-injected side as well as in the scramble-adenovirus-injected side. Scale bar, 1 min. (C,D) Summarized effects of scramble- and *oa1*-adenovirus vectors on the depressor (ΔMBP) and bradycardic (ΔHR) responses to DOPA and glutamate. *$P < 0.05$, compared with the levels of the scramble side ($n = 5$).

obtained with DOPA CHE (data not shown). Scatchard plot analysis showed [^{3}H]-DOPA binding with a K_D value of 79.1 ± 18.2 μM (Figure 5A,B). DOPA CHE displaced the [^{3}H]-DOPA binding in a concentration-dependent manner (Figure 5C). The estimated K_i value of DOPA CHE was 135.9 ± 40.4 μM. It is therefore to be noted that the [^{3}H]-DOPA binding to OA1 expressed in CHO cells was of low affinity. However, this may not reflect the nature of OA1 in neuronal cells because the possibility of a low expression of mature OA1 in a heterologous CHO expression system cannot be excluded.

DOPA increased intracellular Ca^{2+} concentrations ($[Ca^{2+}]_i$) in CHO cells expressing OA1 (Lopez *et al.*, 2008). However, $[Ca^{2+}]_i$ responses to DOPA were barely detectable in CHO cells under our experimental conditions (data not shown). We tried to detect $[Ca^{2+}]_i$ responses to DOPA in ARPE-19 cells, which are derived from retinal pigment epithelium (Dunn *et al.*, 1996) and found that 10 μM DOPA reproducibly and reliably induced the $[Ca^{2+}]_i$ response in ARPE-19 cells expressing OA1 (Figure 5D and upper panels in 5E). DOPA produced no effect in the non-transfected cells. This response was suppressed by pretreatment with DOPA CHE (Figure 5F,G and lower panels in 5E). DOPA CHE alone produced no effect in ARPE-19 cells expressing OA1 (Figure 5F). These findings indicate that DOPA CHE acts as a competitive antagonist of DOPA.

DOPA CHE microinjected into the NTS against phenylephrine-induced bradycardia

To test for a tonic function of OA1 in the baroreceptor reflex, we examined the effect of DOPA CHE bilaterally injected into the NTS on phenylephrine-induced bradycardic response. DOPA CHE (1 μg) alone unilaterally microinjected into the NTS elicited no effect. DOPA CHE antagonized depressor and bradycardic response to DOPA (Figure 6A). Phenylephrine infusion induced a rise in BP and bradycardia (Figure 6C,D). The maximal changes in HR and BP were –37.6 ± 3.6 beats·min^{-1} and 26.9 ± 3.2 mmHg, respectively. We then performed bilateral injections of DOPA CHE into the NTS to examine its effect on the reflex bradycardia induced by phenylephrine infusion (Figure 6B–D). After treatment of DOPA CHE, phenylephrine-induced maximal changes in HR and BP were –2.8 ± 3.0 beats·min^{-1} and 25.3 ± 2.9 mmHg respectively (Figure 6C,D). No changes were observed when saline

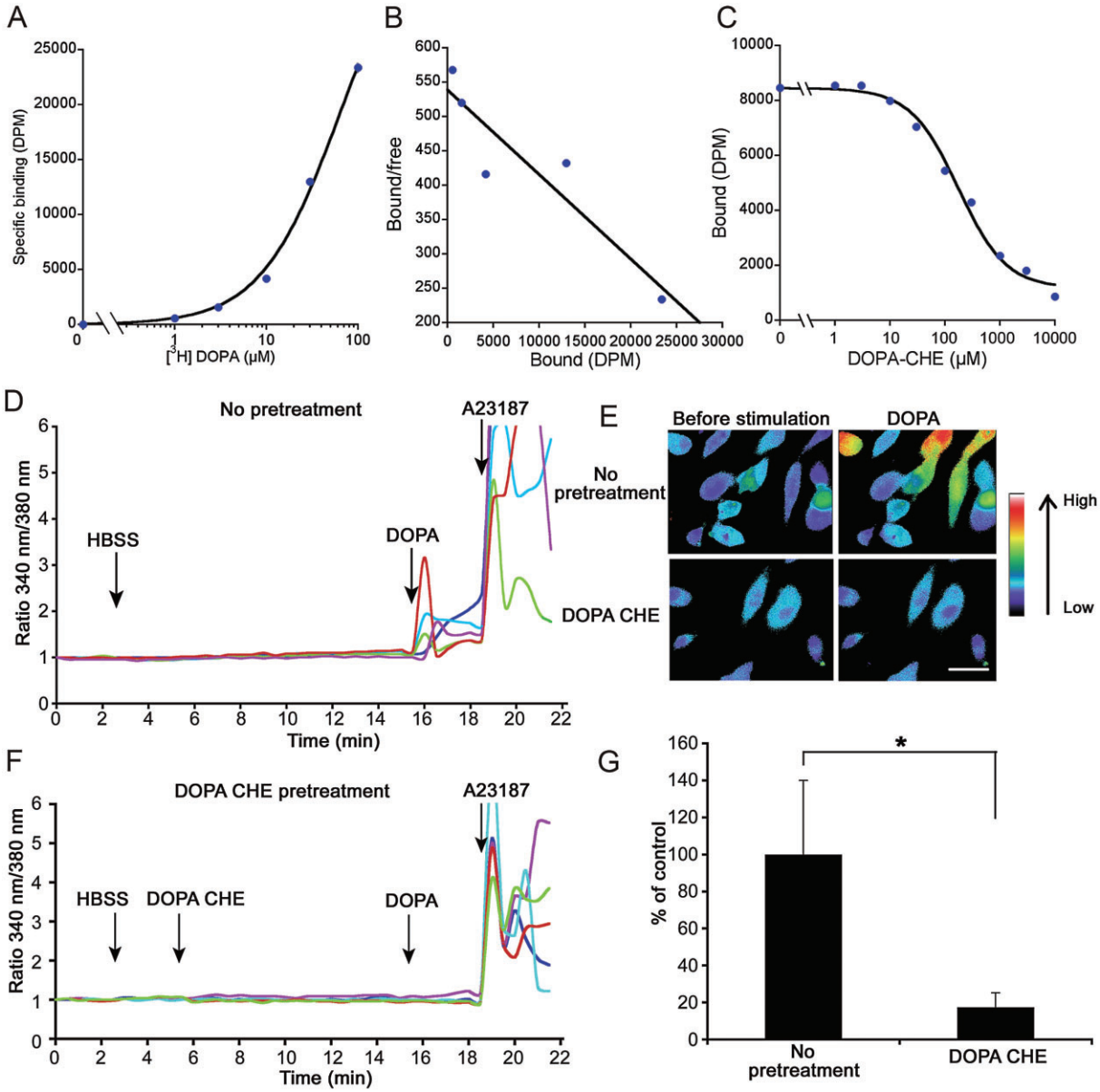

Figure 5

(A,B) [^{3}H]-DOPA binding on CHO cells expressing OA1-EGFP. Specific binding was obtained by the subtraction of the binding value with 10 mM DOPA CHE from the total binding. One typical example is shown. (A) Saturation curve. (B) Scatchard plot. The estimated K_D is 81.3 μM from this experiment. (C) Competitive inhibition of 10 μM [^{3}H]-DOPA binding to OA1-EGFP with various concentration of DOPA CHE. Results indicate that DOPA CHE and DOPA compete for the same OA1 binding site. The estimated K_i for DOPA CHE from this experiment is 155.1 μM. (D–G) Representative traces of [Ca^{2+}]i during the time course of the standard experimental protocol in ARPE-19 cells transfected with mouse OA1-mCherry. After establishing a stable baseline, the cells were stimulated with 10 μM DOPA. DOPA CHE (10 μM), when used, was applied 10 min before DOPA application. DOPA CHE alone produced no effect. (D,E: upper panels) were inhibited by DOPA CHE pre-incubation (E,F: lower panels). Calcium ionophore (4-Br A23187) was added to confirm the Ca^{2+} imaging (D,F). (G) Summary data for [Ca^{2+}]i in response to DOPA and DOPA CHE inhibition. Each bar represents the mean change from baseline [Ca^{2+}]i after DOPA stimulation. Data shown are mean ± SEM (n = 5). *P < 0.01, compared with no pre-treatment.

was microinjected bilaterally into the depressor sites of the NTS (data not shown). Recovery from DOPA CHE antagonism was apparent approximately 30 min after the microinjection (Figure 6). These results suggest that OA1, a DOPA CHE-sensitive recognition site(s), was involved in phenylephrine-induced bradycardic response in the NTS.

Discussion

We proposed some time ago that DOPA itself was a neurotransmitter (Misu and Goshima, 1993). Evidence in support of this proposal included the neurons that contain DOPA as an end product in the CNS (Misu *et al.*, 2003). Further, DOPA

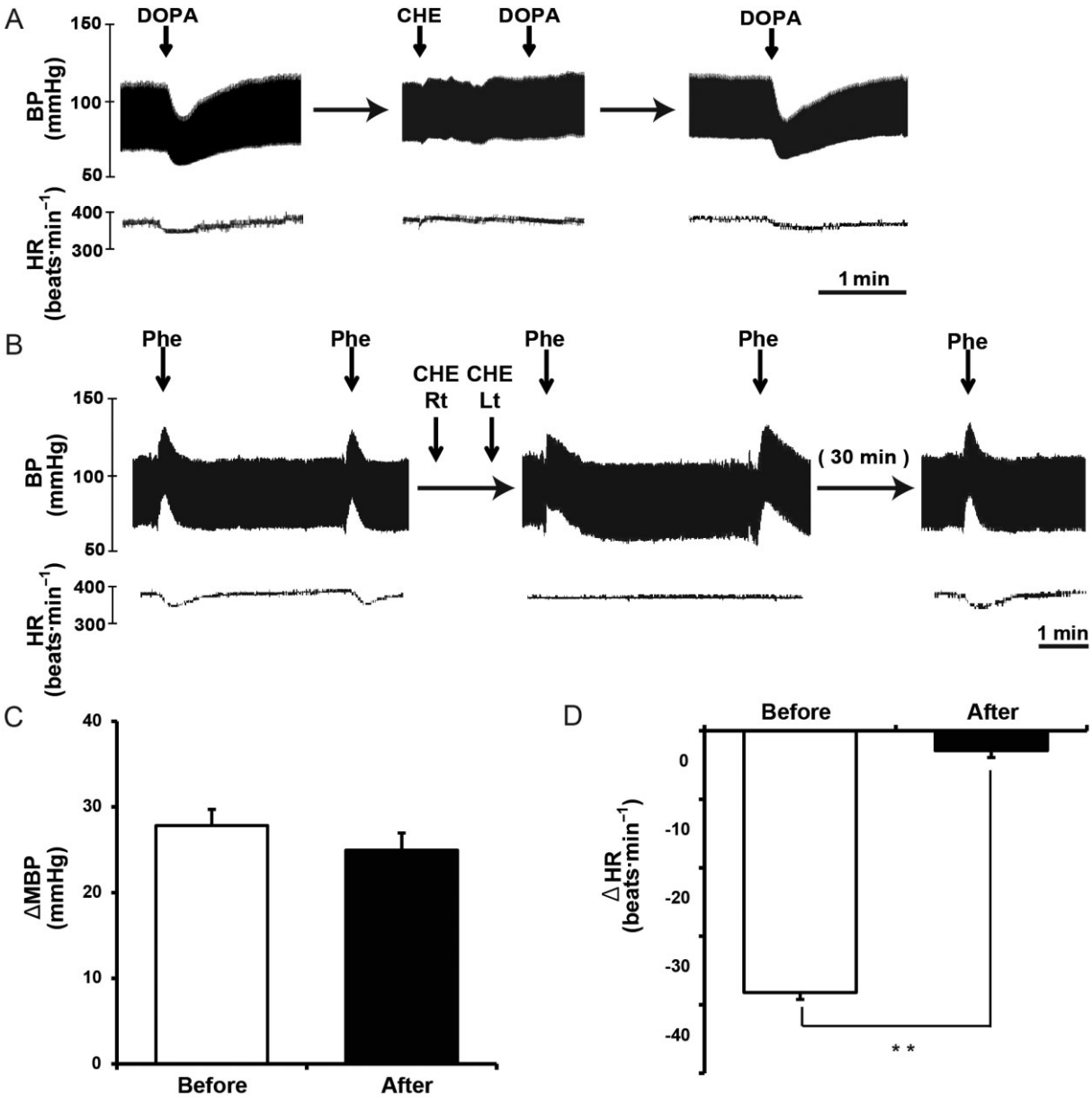

Figure 6

(A) A typical trace of the effect of DOPA (60 ng) before and after microinjection of DOPA CHE (1 μg) into the NTS of anaesthetized rats on BP and HR. (B) Antagonism by bilateral microinjection (Rt, right; Lt, left) of DOPA CHE (1 μg) against bradycardic responses to i.v. infusion of phenylephrine (Phe) (15 μg 10 mL^{-1}·min^{-1}) for 15 s. Scale bar, 1 min. (C,D) Summarized data on Phe-induced changes in BP (C, ΔBP) and HR (D, ΔHR) before and after DOPA CHE. **$P < 0.01$, compared with the levels before DOPA CHE microinjection ($n = 6$).

was released from neurons *in vitro* and *in vivo* in a transmitter-like manner (Goshima *et al.*, 1988). Also, DOPA induced pre- and postsynaptic responses during inhibition of AADC and these actions were antagonized by DOPA antagonists such as DOPA methyl ester or DOPA CHE (Goshima *et al.*, 1986; Kubo *et al.*, 1992; Furukawa *et al.*, 2000). However, specific receptor(s) that could mediate these effects of DOPA had not been identified.

In the present study, we have demonstrated the distribution of OA1-immunoreactive cells in the NTS, and OA1 silencing in the NTS, using the recombinant adenovirus containing the shRNA sequences for *oa1*-specific RNAi, attenuated the depressor and bradycardic responses to DOPA (Figure 4). The analysis of the specific binding of [^{3}H]-DOPA and DOPA-induced $[Ca^{2+}]_i$ changes in OA1-expressing cell lines showed that DOPA CHE acted as a competitive antagonist against OA1. DOPA CHE, when microinjected into the NTS, suppressed bradycardic responses to phenylephrine. These findings clearly demonstrated that OA1 is a receptor of DOPA that mediates depressor and bradycardic responses to DOPA in the NTS (Misu and Goshima, 1993; Misu *et al.*, 2003).

Among many candidates, glutamate is believed to be the neurotransmitter of the baroreceptor reflex pathway in the NTS. The injection of glutamate into the NTS induces the bradycardic response (Talman *et al.*, 1980), and the baroreceptor reflex is attenuated by microinjection of glutamate antagonists into the NTS (Ohta and Talman, 1994). Sub- or millimolar concentrations of DOPA can also interact with AMPA-type glutamate receptors (Miyamae *et al.*, 1999). Thus, it is important to distinguish between glutamatergic receptor(s) and DOPA-specific receptor(s) in the mediation of DOPA-induced cardiovascular responses. To address this question, we employed RNAi knock-down in the NTS region with a recombinant adenovirus containing effective shRNA for *oa1*. Infection with *oa1*-adenovirus in the NTS suppressed the depressor and bradycardic responses to DOPA. In contrast, glutamate microinjected either into the *oa1*-adenovirus-injected or the scramble-adenovirus-injected sides induced similar depressor and bradycardic responses (Figure 4). This result clearly indicates that OA1 mediated the depressor and bradycardic responses to DOPA but not to glutamate in the NTS.

Does OA1 mediate the baroreceptor reflex in the NTS? A straightforward way to address this question may be to test the baroreceptor reflex following bilateral knock-down of OA1 in the NTS. However, at least in our experimental condition, acute knock-down of OA1 by bilateral injection of *oa1*-adenovirus but not the scramble-adenovirus into the NTS was associated with a high mortality rate. This observation suggests that OA1 in the NTS plays an important role in regulating homeostatic control. At present, the mechanism underlying the effect of OA1 knock-down is unknown. In the present study, we therefore tested the effect of DOPA CHE on the baroreceptor reflex. DOPA CHE antagonizes DOPA-induced depressor and bradycardic response in a competitive manner in anaesthetized rats (Furukawa *et al.*, 2000) but did not interact with the dopamine D_1 and D_2 receptors, α- and β-adrenoceptors or 5-HT_{1A} receptors (Miyamae *et al.*, 1999; Furukawa *et al.*, 2000). In addition, we show that DOPA CHE acts as a competitive antagonist against OA1 in the binding assay and Ca^{2+} imaging analysis in OA1-expressing cells (Figure 5). As expected, bilateral injection of DOPA CHE suppressed phenylephrine-induced bradycardia (Figure 6B,D). Further studies are required to elucidate the function of OA1 in central cardiovascular functions and the baroreceptor reflex.

In addition to acting through its conversion to dopamine, DOPA probably exerts some of its actions by interacting with OA1. For example, our present study argues for the idea that hypotension, one of the major side effects of DOPA in Parkinsonian patients, could be mediated by activation of OA1 (Calne *et al.*, 1970; Watanabe *et al.*, 1970; Hoehn, 1975; Mathias, 2002). The mechanisms underlying DOPA-induced 'wearing off', 'on-off' phenomena and dyskinesia encountered during chronic therapy of Parkinson's disease are not fully understood (Iravani and Jenner, 2011). The significance of OA1 in DOPA therapy in Parkinson's disease is also unknown. Whether these effects of DOPA and those seen under the inhibition of AADC such as presynaptic modulation of catecholamine release (Goshima *et al.*, 1986) or ischaemia-induced delayed neuronal cell death (Misu *et al.*, 2003) are important subjects of future studies.

In conclusion, OA1 mediates the action of DOPA in the rat NTS. This study demonstrates, for the first time, that OA1 mediates physiological and/or pharmacological responses to DOPA in the CNS. Our present findings will provide clues as to the potential mechanism of DOPA action and may lead to a fundamental review of DOPA therapy.

Acknowledgements

We thank T. Okada, M. Fujii, S. Chen, N. Fukuda and S. Naito for excellent technical assistance. We thank Emeritus Professor Misu for his encouragement and constructive input. We also thank Drs K Ogura and I Kimura for discussion. This work was supported by Grants-in-aid from the Ministry of Education, Culture, Sport, Science and Technology of Japan (Y. G.), the Naito Foundation (Y. G.) and the Japanese Smoking Research Foundation (Y. G.).

Conflict of interest

None.

References

Aicher SA, Milner TA, Pickel VM, Reis DJ (2000). Anatomical substrates for baroreflex sympathoinhibition in the rat. Brain Res Bull 51: 107–110.

Alexander SPH *et al.* (2013). The Concise Guide to PHARMACOLOGY 2013/14: Overview. Br J Pharmacol 170: 1449–1867.

Andresen MC, Mendelowitz D (1996). Sensory afferent neurotransmission in caudal nucleus tractus solitarius – common denominators. Chem Senses 21: 387–395.

Aoki R, Yagami T, Sasakura H, Ogura K, Kajihara Y, Ibi M *et al.* (2011). A seven-transmembrane receptor that mediates avoidance response to dihydrocaffeic acid, a water-soluble repellent in *Caenorhabditis elegans*. J Neurosci 31: 16603–16610.

Bartholini G, Burkard WP, Pletscher A (1967). Increase of cerebral catecholamines caused by 3,4-dihydroxyphenylalanine after inhibition of peripheral decarboxylase. Nature 215: 852–853.

Calne DB, Brennan J, Spiers AS, Stern GM (1970). Hypotension caused by L-DOPA. Br Med J 1: 474–475.

Dunn KC, Aotaki-Keen AE, Putkey FR, Hjelmeland LM (1996). ARPE-19, a human retinal pigment epithelial cell line with differentiated properties. Exp Eye Res 62: 155–169.

Furukawa N, Goshima Y, Miyamae T, Sugiyama Y, Shimizu M, Ohshima E *et al.* (2000). L-DOPA cyclohexyl ester is a novel potent and relatively stable competitive antagonist against L-DOPA among several L-DOPA ester compounds. Jpn J Pharmacol 82: 40–47.

Garner A, Jay BS (1980). Macromelanosomes in X-linked ocular albinism. Histopathology 4: 243–254.

Goshima Y, Kubo T, Misu Y (1986). Biphasic actions of L-DOPA on the release of endogenous noradrenaline and dopamine in rat hypothalamic slices. Br J Pharmacol 89: 229–234.

Goshima Y, Kubo T, Misu Y (1988). Transmitter-like release of endogenous 3,4-dihydroxyphenylalanine from rat striatal slices. J Neurochem 50: 1725–1730.

Goshima Y, Nakamura S, Misu Y (1991). L-dihydroxyphenylalanine methyl-ester is a potent competitive antagonist of the L-dihydroxyphenylalanine-induced facilitation of the evoked release of endogenous norepinephrine from rat hypothalamic slices. J Pharmacol Exp Ther 258: 466–471.

Hoehn MM (1975). Levodopa-induced postural hypotension. Treatment with fludrocortisone. Arch Neurol 32: 50–51.

Iravani MM, Jenner P (2011). Mechanisms underlying the onset and expression of levodopa-induced dyskinesia and their pharmacological manipulation. J Neural Transm 118: 1661–1690.

Kilkenny C, Browne W, Cuthill IC, Emerson M, Altman DG (2010). Animal research: Reporting *in vivo* experiments: the ARRIVE guidelines. Br J Pharmacol 160: 1577–1579.

Kubo T, Yue JL, Goshima Y, Nakamura S, Misu Y (1992). Evidence for L-DOPA systems responsible for cardiovascular control in the nucleus tractus solitarii of the rat. Neurosci Lett 140: 153–156.

Lopez VM, Decatur CL, Stamer WD, Lynch RM, McKay BS (2008). L-DOPA is an endogenous ligand for OA1. Plos Biol 6: e236–e236.

McGrath J, Drummond G, Kilkenny C, Wainwright C (2010). Guidelines for reporting experiments involving animals: the ARRIVE guidelines. Br J Pharmacol 160: 1573–1576.

Mathias CJ (2002). Neurodegeneration, Parkinsonian syndromes and autonomic failure. Auton Neurosci 96: 50–58.

Milligan G (2009). G protein-coupled receptor hetero-dimerization: contribution to pharmacology and function. Br J Pharmacol 158: 5–14.

Misu Y, Goshima Y (1993). Is L-DOPA an endogenous neurotransmitter. Trends Pharmacol Sci 14: 119–123.

Misu Y, Kitahama K, Goshima Y (2003). L-3,4-dihydroxyphenylalanine as a neurotransmitter candidate in the central nervous system. Pharmacol Ther 97: 117–137.

Miyamae T, Goshima Y, Shimizu M, Shibata T, Kawashima K, Ohshima E *et al*. (1999). Some interactions of L-DOPA and its related compounds with glutamate receptors. Life Sci 64: 1045–1054.

O'Donnell FE Jr, Hambrick GW Jr, Green WR, Iliff WJ, Stone DL (1976). X-linked ocular albinism. An oculocutaneous macromelanosomal disorder. Arch Ophthalmol 94: 1883–1892.

Ohta H, Talman WT (1994). Both NMDA and non-NMDA receptors in the NTS participate in the baroreceptor reflex in rats. Am J Physiol 267: R1065–R1070.

Okamura H, Kitahama K, Mons N, Ibata Y, Jouvet M, Geffard M (1988). L-DOPA-immunoreactive neurons in the rat hypothalamic tuberal region. Neurosci Lett 95: 42–46.

Schiaffino MV, d'Addio M, Alloni A, Baschirotto C, Valetti C, Cortese K *et al*. (1999). Ocular albinism: evidence for a defect in an intracellular signal transduction system. Nat Genet 23: 108–112.

Sugaya Y, Sasaki Y, Goshima Y, Kitahama K, Kusakabe T, Miyamae T *et al*. (2001). Autoradiographic studies using L-[(14)C]DOPA and L-DOPA reveal regional Na(+)-dependent uptake of the neurotransmitter candidate L-DOPA in the CNS. Neuroscience 104: 1–14.

Sun MK (1996). Pharmacology of reticulospinal vasomotor neurons in cardiovascular regulation. Pharmacol Rev 48: 465–494.

Surace EM, Angeletti B, Ballabio A, Marigo V (2000). Expression pattern of the ocular albinism type 1 (Oa1) gene in the murine retinal pigment epithelium. Invest Ophthalmol Vis Sci 41: 4333–4337.

Talman WT, Perrone MH, Reis DJ (1980). Evidence for L-glutamate as the neurotransmitter of baroreceptor afferent nerve-fibers. Science 209: 813–815.

Watanabe AM, Chase TN, Cardon PV (1970). Effect of L-DOPA alone and in combination with an extracerebral decarboxylase inhibitor on blood pressure and some cardiovascular reflexes. Clin Pharmacol Ther 11: 740–746.

Yue JL, Okamura H, Goshima Y, Nakamura S, Geffard M, Misu Y (1994). Baroreceptor-aortic nerve-mediated release of endogenous L-3,4-dihydroxyphenylalanine and its tonic depressor function in the nucleus tractus solitarii of rats. Neuroscience 62: 145–161.